A R C H I V E S O F M E T A L L U R G Y A N D M A T E R I A L S
Volume 56 2011 Issue 4
DOI: 10.2478/v10172-011-0143-4

M. DUDEK*, M. MOSIAŁEK**,***, G. MORDARSKI**,***, R.P. SOCHA**, A. RAPACZ-KMITA****

IONIC CONDUCTIVITY OF THE CeO_2-Gd_2O_3-SrO SYSTEM

PRZEWODNICTWO JONOWE W UKŁADZIE CeO_2-Gd_2O_3-SrO

The Pechini method was used to synthesize nanopowders of CeO_2-based solid solutions with the formula $Ce_{0.8-x}Gd_{0.2}Sr_xO_{2-\delta}$ for 0<x<0.1. All powders and sinters were found to be ceria-based cubic solid solutions. The electrical properties of the ceria-based solid solutions were studied by the a.c impedance spectroscopy method within a temperature range of 200-700°C.

It was found that by adding a small amount of cation Sr^{2+} into the solid solution $Ce_{0.8-x}Gd_{0.2}Sr_xO_{2-\delta}$<x<0.05 allowed us to slightly improve the ionic conductivity of a $Ce_{0.8}Gd_{0.2}O_{2\delta}$ oxide electrolyte. Selected materials from the CeO_2-Gd_2O_3-SrO system were tested as oxide electrolytes in the solid oxide fuel cells operating in a temperature range of 600-700°C. Two kinds of cathode oxide materials were used: monophase $Sm_{0.5}Sr_{0.5}CoO_3$ and the composite cathode $Sm_{0.5}Sr_{0.5}CoO_3$-5% wt. Ag. It was found that a solid oxide fuel cell with a $Ce_{0.78}Gd_{0.2}Sr_{0.02}O_2$ electrolyte exhibited higher power and current densities compared to IT-SOFC involving $Ce_{0.8}Gd_{0.2}O_2$ as an oxide electrolyte. The utilization of a $Sm_{0.5}Sr_{0.5}CoO_3$-5% wt. composite cathode into IT-SOFC could be an additional factor improving its performance in the temperature range 600-700°C.

Keywords: solid oxide electrolytes, ceria-based solid solutions, co-doping, solid oxide fuel cell

Jednofazowe proszki roztworów stałych $Ce_{0.8-x}Gd_{0.2}Sr_xO_{2-\delta}$dla 0<x<0.1 syntezowano metodą Pechiniego. Właściwości elektryczne tych spieków zbadano metodą spektroskopii impedancyjnej w temperaturach od 200 do 700°C. Na podstawie tych badań stwierdzono, że wprowadzenie SrO do roztworu stałego $Ce_{0.8-x}Gd_{0.2}Sr_xO_{2-\delta}$ <x<0.05 prowadzi do podwyższenia przewodności jonowej elektrolitu tlenkowego $Ce_{0.8}Gd_{0.2}O_{2-\delta}$. Wybrane materiały z układu CeO_2-Gd_2O_3-SrO przetestowano jako elektrolity tlenkowe w dwukomorowym stałotlenkowym ogniwie paliwowym pracującym w temperaturach od 600-700°C. Jako materiały katodowe zastosowano: jednofazowy $Sm_{0.5}Sr_{0.5}CoO_3$ oraz kompozytowy $Sm_{0.5}Sr_{0.5}CoO_3$ zawierający dodatek 5% wag srebra.

W wyniku przeprowadzonych prac doświadczalnych stwierdzono, że zastosowanie elektrolitu tlenkowego $Ce_{0.78}Gd_{0.2}Sr_{0.02}O_2$ w stałotlenkowym ogniwie paliwowym pozwala na otrzymanie wyższych gęstości prądu oraz mocy w odniesieniu do tego samego ogniwa IT-SOFC lecz zawierającego elektrolit $Ce_{0.8}Gd_{0.2}O_2$. Kolejnym czynnikiem poprawiającym prace tych ogniw w zakresie temperatur 600-700°C może być stosowanie kompozytowych materiałów katodowych zawierających $Sm_{0.5}Sr_{0.5}CoO_3$ z dodatkiem 5% wag. Ag.

1. Introduction

Until now, solid oxide fuel cell systems have been based mainly on yttria-stabilized zirconia (YSZ) ceramics, because of their nearly pure oxygen conductivity in oxidizing and reducing atmospheres as well as good mechanical properties [1,2]. ZrO_2-based electrolytes, however, require high operating temperatures over 900°C in order to maintain high oxygen ionic conductivity. Such high operating temperatures result in large fabrication costs and accelerate the degradation of the fuel cell systems [3].

Ceria – based solid solutions with the formula $Ce_{1-x}M_xO_{2-\delta}$, M = Gd, Sm, Y and 0.1<x<0.3 are considered as potential candidates for application as oxide electrolytes for solid oxide fuel cells (SOFCs) operating with in a temperature range of 600-800°C [4]. Materials co-stabilized with Gd_2O_3 or Sm_2O_3 and other trivalent cations such as La^{3+}, Nd^{3+}, Y^{3+}, Bi^{3+}, Nd^{3+} or divalent cations Ca^{2+}, Mg^{2+}, Sr^{2+}, depending on chemical composition, have generally improved ionic conductivity

* AGH – UNIVERSITY OF SCIENCE AND TECHNOLOGY, FACULTY OF FUELS AND ENERGY, 30-059 KRAKÓW, 30 MICKIEWICZA AV., POLAND
** INSTITUTE OF CATALYSIS AND SURFACE CHEMISTRY PAS, 30-239 KRAKÓW, 8 NIEZAPOMINAJEK STR., POLAND
*** INSTITUTE OF PHYSICAL CHEMISTRY PAS, 01-224 WARSZAWA, 44/52 KASPRZAKA STR., POLAND
**** AGH – UNIVERSITY OF SCIENCE AND TECHNOLOGY, FACULTY OF MATERIALS SCIENCE AND CERAMICS, 30-059 KRAKÓW, 30 MICKIEWICZA AV., POLAND

compared to singly doped ceria, although in some cases, deterioration of the ionic conductivity or increased electronic conductivity was observed [5, 6]. The application of co-doped ceria electrolytes into IT-SOFC allowed us to obtain higher power and current densities acquired from this cell compared with the same SOFC utilized as an oxide membrane, single - doped ceria with the formula $Ce_{1-x}M_xO_{2-\delta}$, M = Gd, Sm, Y and 0.1<x<0.3 [7].

Unfortunately, IT-SOFCs operating with H_2 fuel usually experience cell performance losses, mainly arising from the cathode. One of the methods used to improve cathode performance is to modify the oxide electrode with noble metals. Ag metal is a promising electrocatalytic material for oxygen reduction reactions.

Sakito, et al. [8] studied the electrochemical properties of a $La_{0.8}Sr_{0.4}Co_{0.2}Fe_{0.8}O_3$- Ag composite cathode. They found that the peak power density of the test cell considerably increased to 0.42W/cm^2 at 530°C by addition of 18 % vol. silver. V.Haanappel, D.Rutenbeck, et al [9] observed that the addition of silver to $La_{0.7}Sr_{0.3}CoO_3$ and $La_{0.7}Sr_{0.3}MnO_3$ cathodes resulted in a significant improvement of electronic conductivity and electrocatalytic activity – for oxygen reduction reaction. Studies have also proved that Ag-particles with a relatively small size and homogenous dispersion always produce an enlarged reaction area, which leads to improved catalytic activity [10-12].

The aim of this work was to examine the possibility of improving the ionic conductivity of a solid electrolyte $Ce_{0.8}Gd_{0.2}O_{2-\delta}$, by partial substitution of Ce^{4+} by Sr^{2+}into the solid solution $Ce_{0.8-x}Gd_{0.2}Sr_xO_{2-\delta}$ and their application in a solid oxide fuel cell operating with Ag-$Sm_{0.5}Sr_{0.5}CoO_3$ as a composite cathode.

2. Materials preparation

The starting materials were: $Ce(NO_3)_3{\cdot}6H_2O$, $Gd(NO_3)_2{\cdot}6H_2O$ (99.9 %), $Sr(NO_3)_2{\cdot}4H_2O$ citric acid and ethylene glycol (99.9% Aldrich). The reagents were mixed in distilled water in order to prepare ceria–based solid solutions with the formula $Ce_{0.8-x}Gd_{0.2}Sr_xO_{2-\delta}$, 0<x<0.1. Citric acid and ethylene glycol were added to the respective nitrate solutions. The solutions were then evaporated at 70°C to obtain hard gels. They were finally calcined at 900°C for 1h and then rotary-vibratory milled with a zirconia grinding media in dry ethanol. The granulated powders were cooled and isostatically pressed under 200 MPa with 5% wax-water emulsion added as a lubricant. The pellets were sintered for 2 h at 1500°C. The cathode powder $Sm_{0.5}Sr_{0.5}CoO_3$ was also prepared by the Pechinni method [13].

2.1. Apparatus and methods investigations of physicochemical and electrochemical properties

The phase composition of all powders and sintered bodies were identified by X-ray diffraction analysis based on the ICDD data base. XRD measurements were done using the Panalytical X'Pert Pro system with monochromatic Cu K_a radiation. Lattice parameters of the identified phases were determined using the Rietveld refinement method. The mean crystalline size (d_{hkl}) of the CeO_2-based powders was calculated according to the Scherrer formula. Specific surface areas were measured by multipoint nitrogen adsorption at –196°C (Quantachrome Nova 1200). The BET adsorption model was involved to calculate particle sizes. Green samples were characterized by pore size distribution measurements (Quantachrome, PoreMaster). Transmission electron microscopy (AEM CM20 Philips) combined with EDS system was used to characterize the morphology and chemical composition of the $Ce_{1-x}Gd_{0.2}Sr_xO_{2-\delta}$0<x<0.1 solid solutions powders. Scanning electron microscopy (NovaNano SEM) eqquiped with an EDX analyzing system was used to observe the microstructure of samples sintered. The apparent density of the sintered bodies was measured by the Archimedes method. Ionic conductivity measurements were performed by the a.c impedance spectroscopy method within a temperature range from 200-800°C in static air. The selected ceria–based samples were tested as solid electrolytes in a two-chamber solid oxide fuel cell (SOFC). An anode (50% wt. NiO-20GDC) powder (supplied by Fuel Cell Materials, USA) was mixed with terpineol and ethyl cellulose to form a slurry, subsequently screen-printed on the side of CeO_2-based electrolytes as the anode, which was thermally heated at 1200°C for 1h. In the next step, $Sm_{0.5}Sr_{0.5}CoO_3$ (SSC) was grounded in a rotary-vibratory mill in dry ethylene alcohol using a zirconia grinding media. The SSC grounded powder was mixed with terpineol and ethyl cellulose to form a slurry. The slurry was screen-printed on the surface of CeO_2-based electrolytes and was first heated at 400°C for 2h to remove organic binders and then heated at 950°C for 4 h with a heating and cooling rate of 2°/min. For the modification of the SSC cathode with silver, a method of nitrate decomposition was applied In general, a $AgNO_3$ solution with a concentration of 0.05mol·dm^{-3} was dropped by a suction pipette with an accuracy of ±0.01 ml and soaked into the porous SSC cathode layer and then heated over a hotplate to evaporate water, followed by firing at 800°C for 4h.

The family of current – voltage (ΔE-I) and current-power (I-P) curves of tested solid oxide fuel

TABLE 1

Average crystalline sizes of CeO_2-powders determined by XRD method and BET specific surface area

Parameter	$Ce_{0.8}Gd_{0.2}O_2$ (20GDC)	$Ce_{0.78}Gd_{0.2}Sr_{0.02}O_2$ (2Sr20GDC)	$Ce_{0.75}Gd_{0.2}Sr_{0.05}O_2$ (5Sr20GDC)	$Ce_{0.7}Gd_{0.2}Sr_{0.1}O_2$ (10Sr20GDC)
crystalline size $d_{(hkl)}$, nm	19.8	23.4	26.2	28.4
particle size $d_{(BET)}$, nm	32.6	40.4	50.2	54.2

cells were also measured by the cyclic voltammetry (CV) method using an Autolab electrochemical station.

3. Results and discussion

XRD diffraction analysis showed that all powders and sinters were found to be cubic ceria-based solid solutions form. The properties of CeO_2-based powders synthesized by this method are collected in Table 1. A small increase of crystalline sizes were detected in all investigated ceria-solid solutions compared to pure CeO_2. In the case of $Ce_{0.8-x}Gd_{0.2}Sr_xO_{2-\delta}$, where $0<x<0.1$, some difference between particle sizes determined by the XRD method $d_{(hkl)}$ or $d_{(BET)}$, which are calculated from surface area measurements, were mentioned. This fact indicates the presence of agglomeration particles in powders, which was previously mentioned during TEM (Fig. 1) observations. All the samples prepared from these powders achieved more than 96% of theoretical density. The typical microstructure of $Ce_{0.78}Gd_{0.2}Sr_{0.02}O_2$ and $Ce_{0.7}Gd_{0.2}Sr_{0.1}O_2$ samples sintered at 1500°C for 2 h are presented in Fig. 2 a-b.

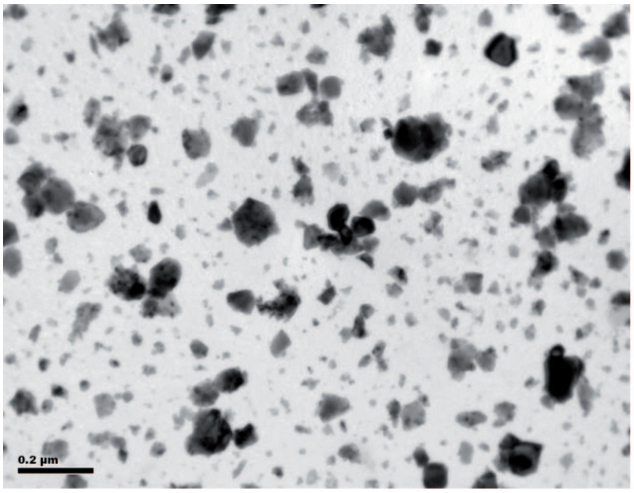

Fig. 1. TEM microphotograph of the $Ce_{0.78}Gd_{0.2}Sr_{0.02}O_{2-\delta}$ rounded powder

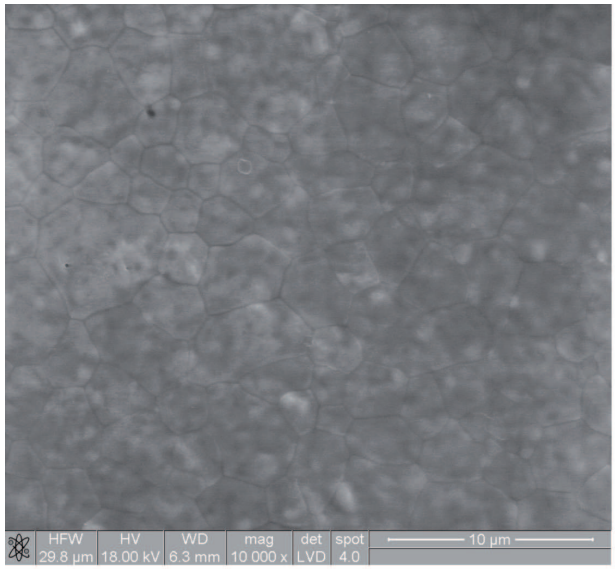

Fig. 2a. The microstructure of a $Ce_{0.78}Gd_{0.2}Sr_{0.02}O_{2-\delta}$ two-hour sintered sample at 1500°C

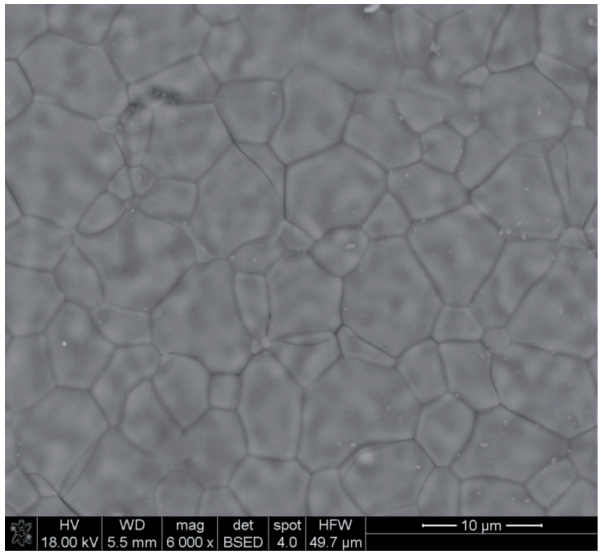

Fig. 2b. The microstructure of a $Ce_{0.7}Gd_{0.2}Sr_{0.1}O_{2-\delta}$ two-hour sintered sample at 1500°C

Processing of microstructural analysis allowed us to determine the average grain size distribution for pure CeO_2 and $Ce_{0.8-x}Gd_{0.2}Sr_xO_{2-\delta}$ solid solutions sintered samples respectively at 1500°C for 2h in air. Fig 3. presents the changes of average grain size vs.

the chemical composition of $Ce_{0.8}Gd_{0.2}Sr_xO_{2-\delta}$ sintered samples obtained starting from powders synthesized by the Pechini method. This microstructural analysis showed that the partial substitution of $Ce^{4+}$by Sr^{2+} into $Ce_{0.8-x}Gd_{0.2}Sr_xO_{2-\delta}$ solid solutions led to a small increase of average grain sizes compared to the starting chemical composition of the $Ce_{0.8}Gd_{0.2}O_{2-\delta}$ sample.

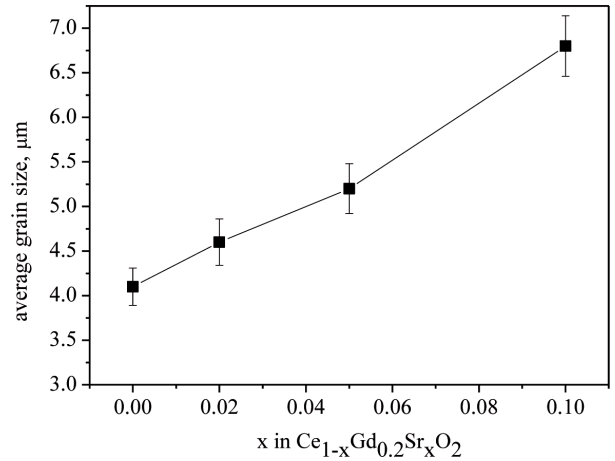

Fig. 3. The dependence of an average grain size vs. the chemical composition of CeO_2-based samples

The changes of lattice constant *a* calculated for the obtained $Ce_{0.8-x}Gd_{0.2}Sr_xO_{2-\delta}$ solid solutions samples are presented in Fig.4. The lattice constant *a*of $Ce_{1-x}Gd_{0.2}SrO_{2-\delta}$ solid solutions increases linearity with the increase of x content. This is due to the different ionic radii of Ce^{4+} (0.96Å) and Sr^{2+} (1.26Å), which agrees with data existing in literature [14].

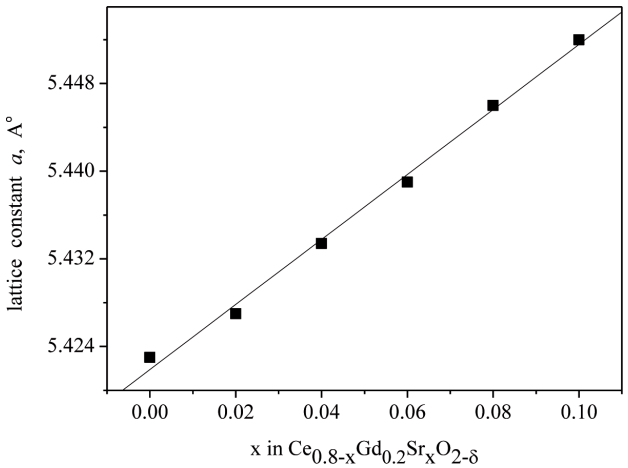

Fig. 4. The changes of lattice cell parameter *a* calculated for $Ce_{0.8-x}Gd_{0.2}Sr_xO_{2-\delta}$ sintered samples

The a.c impedance spectroscopy method was applied to determine the electrical properties of single or co-doped ceria-based samples obtained by the Pechini method (A). Grain and grain boundary resistance arcs for the investigated samples are well resolved up to 400°C (Fig.5). In this case, the equivalent circuit $(R\text{-}CPE)_b$-$(R\text{-}CPE)_{gb}$–$(R\text{-}CE)_{el}$ is used to fit the impedance data to calculate bulk (R_b) and grain boundary resistance (R_{gb}). After 400°C the bulk arc is not well resolved due to a decrease in the relaxation time and its shift towards higher frequency regions, exceeding the equipment limit [15]. In this case, a $R_b(R\text{-}CPE)_{gb}$-$(R\text{-}CPE)_{el}$ equivalent circuit is used to fit the data.

The Arrhenius plot, of the bulk conductivity (σ_b) for $Ce_{0.8}Gd_{0.2}O_{2-d}$ (20GDC), $Ce_{0.78}Gd_{0.2}Sr_{0.02}O_{2-\delta}$ (2Sr20GDC) and $Ce_{0.75}Gd_{0.2}Sr_{0.05}O_{2-\delta}$(5Sr20GDC) is shown (Fig.6.) in lig(σT) v.s 1/T coordinated. These results indicate that the co-doped ceria $Ce_{0.78}Gd_{0.2}Sr_{0.02}O_2$ exhibits slightly higher values of bulk conductivity compared to the $Ce_{0.8}Gd_{0.2}O_{2-\delta}$ sample. Temperature dependence σ can be expressed as:

$$\sigma = \frac{\sigma_o}{T}\exp\left(\frac{\Delta H_m + \Delta H_a}{kT}\right) \qquad (1)$$

where σ_o (in K $\Omega^{-1}\cdot m^{-1}$) is a pre-exponential factor, k – is a Boltzman constant and ΔH_m , ΔH_a, are the migration enthalpy of the oxygen ion and the associated enthalpy of the defect complex.

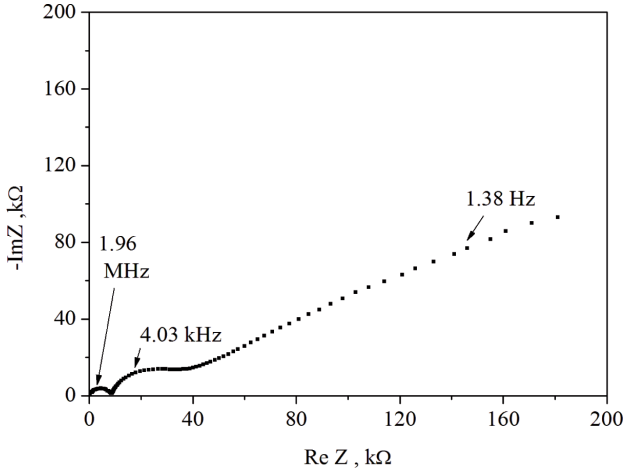

Fig. 5. The impedance spectra recorded at 300°C for $Ce_{0.78}Sr_{0.02}Gd_{0.2}O_{2-\delta}$ ample

Kilner, *et al.* [16] indicated that the association energy of oxygen vacancies is increased by the ionic – radius mismatch between the dopant cation and the host element. It is inferred that the ionic conductivity in fluorite oxides could be enhanced by a decrease of this ionic – radius mismatch. Thus, to enhance the grain conductivity, minimization of the association of defects is required. As expressed before, this association energy is a function of the coulombic attraction between oxygen vacancies and the elastic strain – present in the lattice [17].

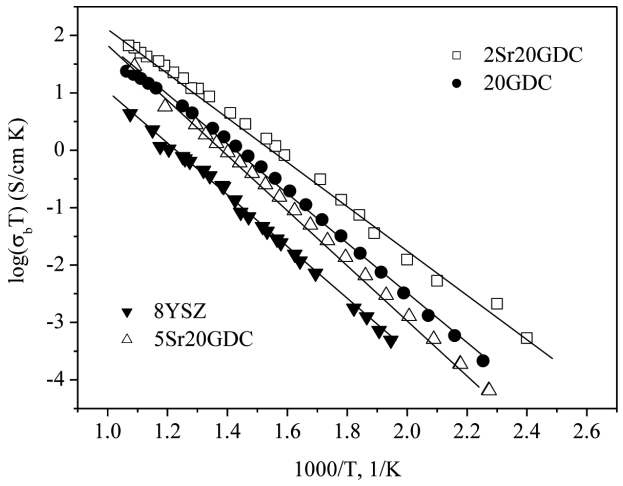

Fig. 6. The log (σ_bT) vs. 1000/T determined for 8% mol Y_2O_3 in ZrO_2 (8YSZ), $Ce_{0.8}Gd_{0.2}O_{2-\delta}$ $Ce_{0.78}Sr_{0.02}Gd_{0.2}O_{2-\delta}$ (2Sr20GDC) and $Ce_{0.75}Sr_{0.05}Gd_{0.2}O_{2-\delta}$5Sr20GDC) samples.

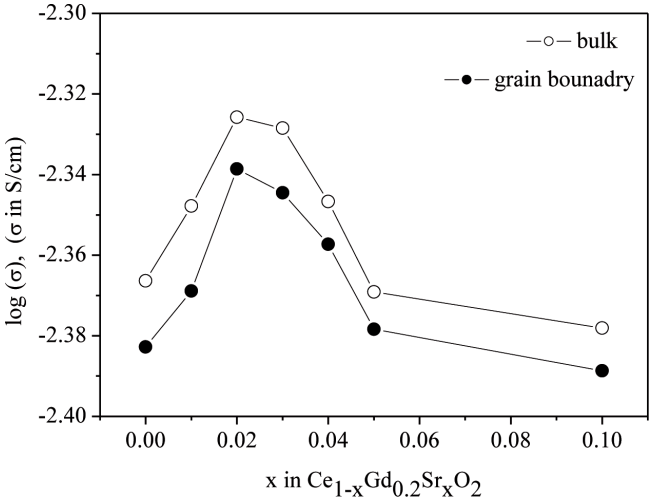

Fig. 7. Bulk and grain bounadry conductivity as a function of composition in $Ce_{0.8-x}Gd_{0.2}Sr_xO_{2-\delta}$ samples at 600°C

Fig. 7 shows the bulk or grain boundary conductivity of co-doped ceria with Sr^{2+} and Gd^{3+} as a function of dopant concentration at 600°C. At a lower dopant concentration of Sr^{2+}(up to x =0.02), the bulk conductivity reaches maximum values and then decreases while increasing the dopant concentration. Analysis of the energy activation (Fig.8) process is also performed to indicate the minimum correspondence to maximum conductivity. The change of activation energy could be attributed to an order – disorder transistion of the oxygen sub-lattice [18,19]. The decrease in activation energy is due to the presence of attractive interactions between cations and oxygen vacancies. Also, with increasing dopant concentration levels, defects associated with oxygen vacancies and dopant cations can change from dimers to trimers and then defect clusters, consequently resulting in high binding energy, which is responsible for the increase of energy activation. In addition, some microdomains of possible ordered intermediate phases could also form, as compared to samples sintered at 1500°C. The possible formation of $SrCeO_3$ should be also considered as one of the main reasons of a decrease in conductivity, although X-ray diffraction does not indicate the presence of $SrCeO_3$ as a second phase [20]. Another problem associated with the final ceramic microstructure is the rather low conductivity of the grain boundary (σ_{gb}), when compared to that of the corresponding bulk. This fact is attributed to the presence of impurities located in the grain boundary, which lowers ionic mobility [21].

The $Ce_{0.8}Gd_{0.2}O_{2-\delta}$ and $Ce_{0.78}Gd_{0.2}Sr_{0.02}O_{2-\delta}$ amples were chosen for further investigations as components for solid oxide fuel cells operated with hydrogen as a fuel.

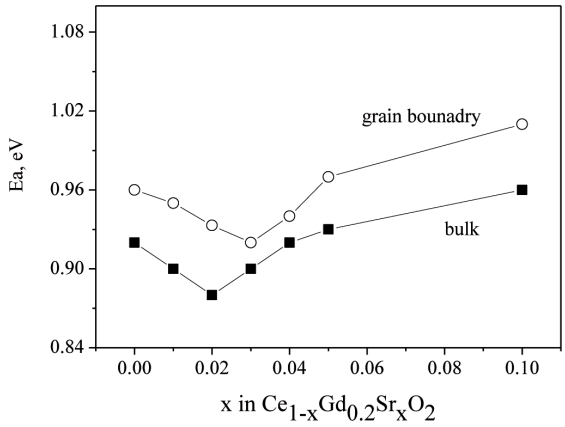

Fig. 8. Activation energy of bulk and grain boundary conductivity of $Ce_{0.8-x}Gd_{0.2}Sr_xO_{2-\delta}$ samples

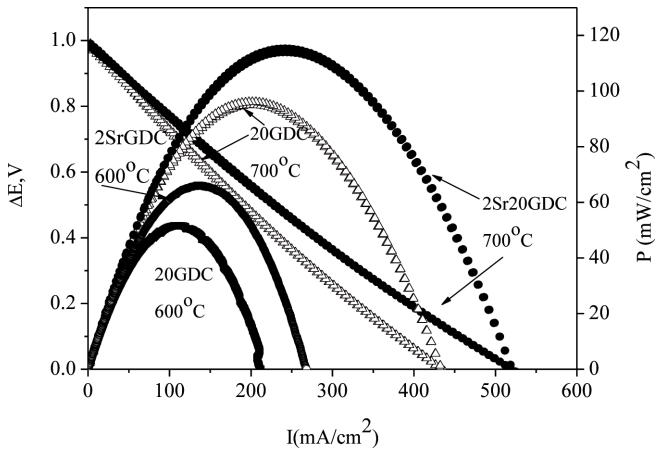

Fig. 9. The family of ΔE-I and P-I curves recorded for (20GDC) and (2Sr20GDC) samples

Fig. 9 shows the performance of SOFC with 20GDC (a) and 2Sr20GDC as electrolytes within a temperature range of 600-700°C. The power (P) density, as well as the current (I) density of SOFC with the $Ce_{0.78}Gd_{0.2}Sr_{0.02}O_{2-d}$ electrolyte, reached higher values than the same SOFC involving the $Ce_{0.8}Gd_{0.2}O_{2-\delta}$ elec-

trolyte. This fact could be attributed to a decrease of the resistance of the cell. As can be seen, the utilization of the solid oxide electrolyte with higher ionic conductivity allowed us to reduce ohmic losses during IT-SOFC performance.

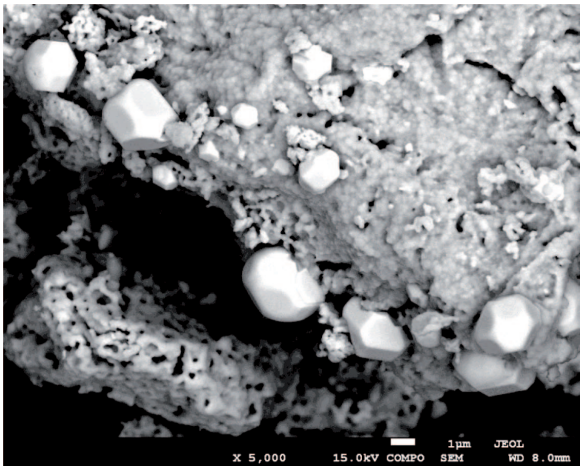

Fig. 10. The SEM microphotograph of the $Sm_{0.5}Sr_{0.5}CoO_3$-5 %wt.Ag composite cathode

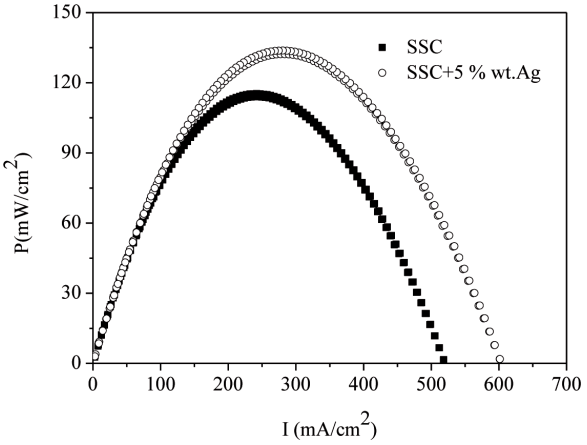

Fig. 11. The family of P-I curves recorded for IT-SOFC with $Ce_{0.78}Sr_{0.02}Gd_{0.2}O_2$ as a solid electrolyte with monophase cathode $Sm_{0.5}Sr_{0.5}CoO_3$(SSC) or $Sm_{0.5}Sr_{0.5}CoO_3$+5% wt.Ag at temperature 700°C

The second idea of improving the power and current densities acquired from IT-SOFC with $Ce_{0.78}Gd_{0.2}Sr_{0.02}O_2$ could be through the utilization of SSC-Ag as a composite cathode. Fig. 10. presents the SEM microphotograph of the Ag-$Sm_{0.5}Sr_{0.5}CoO_3$ obtained composite cathode. As can be seen, the Ag-SSC cathode is porous, and Ag particles about 0.4 to 2μm are randomly distributed on the surface of SSC cathode materials. Fig. 11. presents the family of curves (ΔE-I and P-I) recorded for IT-SOFC with a 2Sr20GDC electrolyte and a SSC or SSC-Ag cathode within a temperature range of 600-700°C. As can be seen, an increase of power (P) and current density (I) was observed for IT-SOFC with 2Sr20GDC with a SSC-Ag composite cathode compared to the same IT-SOFC involving only monophase SSC material.

4. Conclusions

Single-doped ceria, or co-doped ceria CeO_2–Gd_2O_3–SrO materials, were successfully prepared from powders both obtained by the Pechini method. It has been stated that the introduction of strontium into $Ce_{1-x}Gd_{0.2}Sr_xO_2$ solid solutions leads to ionic conductivity enhancement compared with only gadolina – doped ceria. The application of composite cathode oxide materials involving $Sm_{0.5}Sr_{0.5}CoO_3$-Ag also improves the performance of IT-SOFC operating with a co-doped ceria electrolyte.

Acknowledgements

This work was sponsored by the Ministry of Science and Higher education No. 6166/B/T02/2010/38.

REFERENCES

[1] J.W Fergus, Electrolytes for solid oxide fuel cells, J. Power Sources **189**, 30-40 (2006).
[2] A. Pawłowski, M.M. Bućko, Z. Pędzich, Microstructure and properties of ion conductors in the ZrO_2-Y_2O_3-MgO system as an effect DIGM process, Archives of Metallurgy **44** (4), 375-384 (1999).
[3] N.Q. Minh, Ceramic fuel cell, Journal of the American Ceramic Society **73**, 563-588 (1993).
[4] H. Inaba, H. Tagawa, Ceria-based electrolytes Solid State Ionics **83**, 1-16 (1996).
[5] T. Mori, T. Ikegami, H. Yamamura, Application of a Crystallographic Index for Improvement of the Electrolytic Properties of the CeO_2-Sm_2O_3 System J. Electroch. Soc. **146** (12), 4380-4385 (1999).
[6] S. Dikmen, Effect of co-doping with Sm^{3+}, Bi^{3+}, La^{3+} and Nd^{3+} on the electrochemical properties of hydrotermally prepared gadolinium doped ceria ceramics, J. Alloys Compd **491** 106-112 (2010).
[7] S. Ramesh, V. Kummar, P. Kistaih, C. Reddy, Preparation and characterization and thermoelectrical properties of co-doped $Ce_{0.8-x}Sm_{0.2}Ca_xO_{2-d}$ materials Solid State Ionics **181**, 86-91 (2010).
[8] Y. Sakito, A. Hirano, N. Imanishi, Y. Takeda, O. Yamamoto, Y. Liu, Silver inflitatred $La_{0.6}Sr_{0.4}Co_{0.2}Fe_{0.8}O_3$ cathodes for intermediate temperature solid oxide fuel cells, Journal of Power Sources **182**, 476-481 (2008).
[9] V. Haanappel, D. Rutenbeck, A. Mai, S. Uhlenbruck, D. Sebold, H. Wesemeyer, B. Röwekamp, C. Tropartz, F.Tiez, The influence of noble-metal-containing cathodes on the elec-

trochemical performance of annode – supported SOFCs, Journal of Power Sources **130**, 119-128 (2004).

[10] S.P. Simmer, M.D. Anderson, J.W. Templeton, J. Stevenson, Silver-perovskite composite cathodes via mechanofussion, Journal of Power Sources **168**, 236-239 (2007).

[11] M. Sahibzda, S.J. Benson, R.A. Rudkin, J.A. Kilner, Pd-promoted $La_{0.6}Sr_{0.4}Co_{0.2}Fe_{0.8}O_3$ cathodes, Solid State Ionics **113-115**, 285-290 (1998).

[12] Q. Li, Li. Sun, Li. Huo, H. Zhao, J. Grenier, Electrochemical performance of $La_{1.6}Sr_{0.4}NiO_4$-Ag composite cathodes for intermediate temperature solid oxide fuel cells, Journal of Power Sources **196**, 1712-1716 (2011).

[13] Ch. Xia, W. Rauch, F. Chen, M. Liu, $Sm_{0.5}Sr_{0.5}CoO_3$ cathodes for low temperature SOFCs, Solid State Ionics **149**, (2002) 11-19.

[14] R.P Shannon, T. Prewitt, Effective Ionic Radii in Oxides and Fluorides Acta Crystalographica **B25**, 925 (1969).

[15] A.F. Orliukas, A. Kezionis, E. Kazakevicius, Impedance spectroscopy of solid electrolytes in the radio frequency range, Solid State Ionics **176**, 25-28, 2037-2043 (2005).

[16] J.A. Kilner, Fast oxygen transport in acceptor doped oxides Solid State Ionics **129**, 13-23 (2000).

[17] B.C.H. Steele, Appriasal of $Ce_{1-y}Gd_yO_{2-y/2}$ electrolytes for IT-SOFC operation at 500°C, Solid State Ionics **129**, 95-110 (2000).

[18] J. Guor-Nin, H. Ta-Jen, Chung-Liang, Effect of temperature and dopant concentration on the conductivity of samaria-doped ceria electrolyte. Journal of Solid State Electrochem **6**, 225-230 (2002).

[19] P.J. Schlichta, A crystalographic search program for oxygen-conducting electrolytes, Solid State Ionics **28-30**, 480-487 (1988).

[20] P. Seok, S.B. Lee, D.S. Kim, J.H. Lee, D. Kim, H. Park, Improvment of grain – boundary conduction in gadolina – doped ceria by the addition of CaO, Electrochem. Solid-State Lett. (9), A399-A402 (2006).

[21] H. Park, G. Auchterlonie, J. Drennand, Mitigation of Highly resistive grain-boundary phase in gadolina – doped ceria by the addition of SrO, Electrochem. Solid-State Lett. **10** (5) B91-B95 (2007).

Received: 20 March 2011.